Natural Hazards (2024) 120:7173–7193
https://doi.org/10.1007/s11069-024-06474-8

ORIGINAL PAPER

River-damming landslides during the 1960 Chile earthquake (M9.5) and earlier events: implications for risk assessment in the San Pedro River basin

Cristian Araya-Cornejo[1,2] · Matías Carvajal[3,4] · Daniel Melnick[4,5] · Jasper Moernaut[6] · César Araya[7] · Felipe González[8]

Received: 16 June 2023 / Accepted: 29 January 2024 / Published online: 10 March 2024

Abstract
Damming rivers by landslides and ensuing outburst flooding is a common and potentially hazardous phenomenon worldwide, especially in tectonically active regions. Remarkable examples are the damming of the upper course of the San Pedro River (SPR) in south Chile during the 1960 Chile earthquake (M9.5) and its predecessor in 1575. Outburst floods following both events had tragic consequences for downstream communities. Here, we study both events from multiple sources of information, including previously published and newly found historical records, satellite imagery, LiDAR topography, and sedimentological and geomorphological field observations. We present the first detailed geomorphic map of the region. Morphological similarities between ancient deposits at the SPR and those associated with the 1960 earthquake suggest that the SPR has been dammed repeatedly in the past. The steep incision of the SPR and the sediments of glacio-lacustrine origin in the surrounding slopes facilitate the initiation of large landslides. The knowledge gained from studying these past events provides important implications for future risk assessments. We propose that besides large earthquakes, smaller and more frequent earthquakes as well as changes in land use, can also result in river-damming events.

Keywords Earthquakes · Landslide dams · 1960 Chile earthquake · Valdivia · San Pedro River basin · Risk assessment

✉ Cristian Araya-Cornejo
caraya@uahurtado.cl

1 Departamento de Geografía, Universidad Alberto Hurtado, Santiago, Chile

2 Instituto de Geografía, Pontificia Universidad Católica de Chile, Santiago, Chile

3 Instituto de Geografía, Pontificia Universidad Católica de Valparaíso, Valparaiso, Chile

4 Millennium Nucleus The Seismic Cycle Along Subduction Zones, Valdivia, Chile

5 Instituto de Ciencias de la Tierra, TAQUACH, Universidad Austral de Chile, Valdivia, Chile

6 Institute of Geology, University of Innsbruck, Innsbruck, Austria

7 Deprtamento de Geografía, Universidad de Chile, Santiago, Chile

8 Chair for Computational Analysis of Technical Systems, RWTH Aachen University, Aachen, Germany

1 Introduction

Landslides are a recognized hazard in various geologic environments and especially in tectonically active regions (Keefer and Larsen 2007; Marc et al. 2015; Fan et al. 2019, 2020). Their triggering depends on different factors (e.g., heavy rains), with earthquake shaking being the most common (Keefer 1984; Fan et al. 2023). Landslides triggered by earthquakes caused tens of thousands of deaths in densely populated areas (Budimir et al. 2015) and have causes important economic losses (Alexander 2012). Additionally, earthquake-triggered landslides have the potential to trigger cascading hazards like tsunamis as well as river damming, and associated outburst floods (Budimir et al. 2015). Therefore, understanding the characteristics and recurrence of landslides and associated hazard cascades, as well as the factors promoting their occurrence, is important for risk assessments.

Chile is an excellent place to improve such understanding. It is located in one of the most seismically active subduction zones in the world and has one of the highest rates of earthquake occurrences, with an average of two great earthquakes (magnitude (M) = 8+) per century (Ruiz and Madariaga 2018). Although most of the great earthquakes are sourced in the megathrust fault formed by the subduction of the Nazca plate beneath the South America plate (red line in Fig. 1c.), intraplate faults (e.g., within either plate such as those indicated by the brown and green lines in Fig. 1c) have also generated large magnitude events (M > 6) with shaking strong enough to trigger landslides (Antinao and Gosse 2009; Hermanns et al. 2012). The M6.2 2007 shallow crustal earthquake sourced in the Liquiñe-Ofqui strike-slip fault (LOFZ, in Fig. 1c) in south Chile is an example of these earthquakes (Agurto et al. 2012). It triggered multiple landslides (e.g., rock slides, rock avalanches, slumps, slow earth flows, and others) that entered the Aysén Fjord, generating tsunamis that killed about a dozen people (Sepúlveda et al. 2010). This recent event, plus others (e.g., Serey et al. 2019), highlights the urgent need for better understanding earthquake-triggered landslides in Chile and their cascading hazards.

An opportunity to improve the knowledge of landslide science comes from south Chile. The upper course of the San Pedro River (SPR; 39.7° S, 72.4° W), which originates in the Andean Riñihue Lake in south Chile, holds a well-known landslide story. This river and lake received attention after it was dammed by three landslides triggered during the 1960 earthquake (see Sect. 4.3). The deposits that dammed the river were called locally *Taco 3* (hereinafter LT3), *Taco 2* (hereinafter LT2), and *Taco 1* (hereinafter LT1), respectively (Fig. 2c). As water accumulated upstream of the uppermost dam, its pressure increased, posing a time-increasing threat to the downstream population. Fortunately, when the lake level reached about ~ 26 m above its typical level, successful interventions led by the Chilean government with the collaboration of local inhabitants, prevented an imminent dam collapse saving tens of thousands of people (Davis and Karzulovic 1961). A similar story had occurred almost four centuries before, with more tragic consequences. The historical earthquake of 1575, recognized as the predecessor of the 1960 earthquake (Cisternas et al. 2005; Moernaut et al. 2014; Ruiz and Madariaga 2018; Matos-Llavona et al. 2022), also triggered landslides that dammed the SPR (see Sect. 3). However, on that occasion, after months of water accumulation and over ~ 50 m of water-level increase, the dam collapsed and killed hundreds of inhabitants living downstream (Montessus de Ballore 1912).

In this paper, we seek to improve the knowledge of earthquake-triggered landslides by studying the landslide deposits of the 1960 and earlier south Chile earthquakes present in the upper course of the SPR. The knowledge gained from these past events is then used to study the local factors currently controlling landslide generation in the

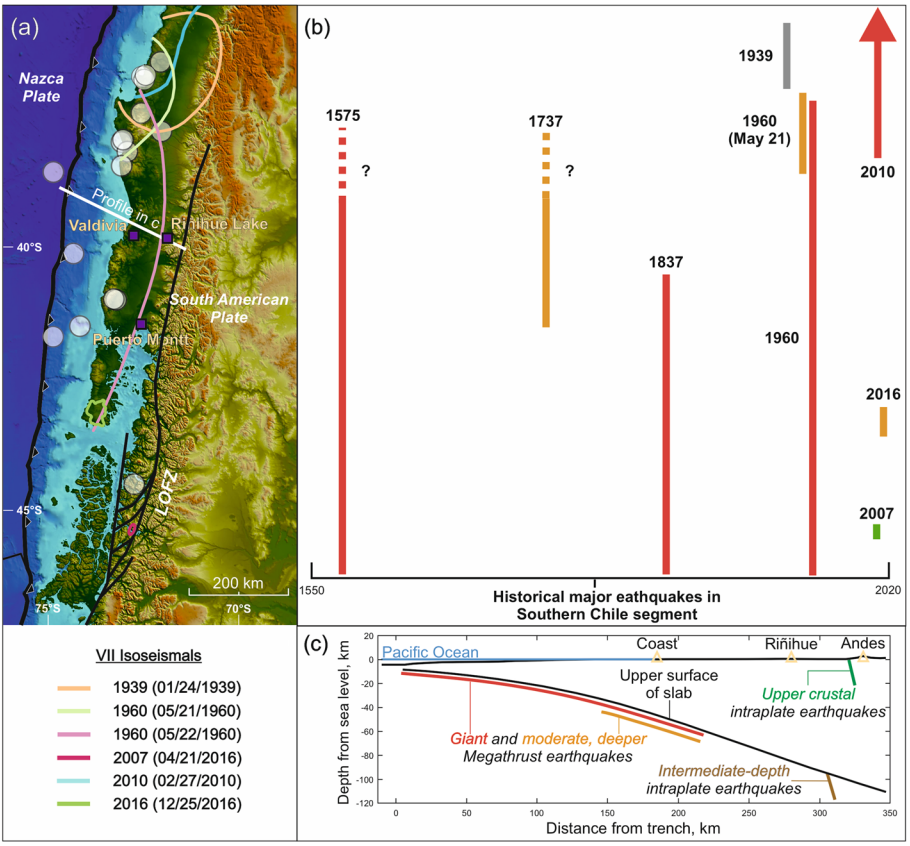

Fig. 1 **a** Location of earthquakes larger than Magnitude 7 that struck South-Central Chile in the historical period 1570–2016 (National Seismological Center of Chile 2019); and Isoseismal VII of the intraplate earthquakes of 1939 (Astroza et al. 2002) and 2007 (Vanneste et al. 2018); and interplate earthquakes of 1960 (21 and 22 of May) (Astroza and Lazo 2010), 2010 (Astroza et al. 2012), and 2016 (USGS 2016). White circles indicate earthquake events with magnitudes apparently over 7 from 1570. **b** Rupture lengths of the most significant, well-investigated earthquakes along the region. The line colors represent the source type of the earthquakes shown in **c**. Orange lines indicate the along-dip location of moderate-size, deeper interplate earthquakes (1737 (Cisternas et al. 2017a), May 21, 1960 (Ruiz and Madariaga 2018), and 2016 (Moreno et al. 2018)). Red lines indicate the along-dip location of great earthquakes rupturing the entire seismogenic width (1575, 1960 (Cisternas et al. 2005; Wils et al. 2020) and 2010 (Moreno et al. 2012)). The green line indicates the approximate location of crustal earthquakes, such as the strike-slip rupture of the 2007 earthquake along the Liquiñe Ofqui Fault Zone (LOFZ) (Agurto et al. 2012). The brown line indicates the approximate location of intermediate-depth earthquakes such as the 1939 intermediate-depth earthquake rupture within the subducted slab (Beck et al. 1998)

SPR and the implications of modern land use on future risk assessment in the area. To this end, we combine multiple sources of information, including field observations, satellite and LiDAR imagery, and previously published and newly found historical accounts.

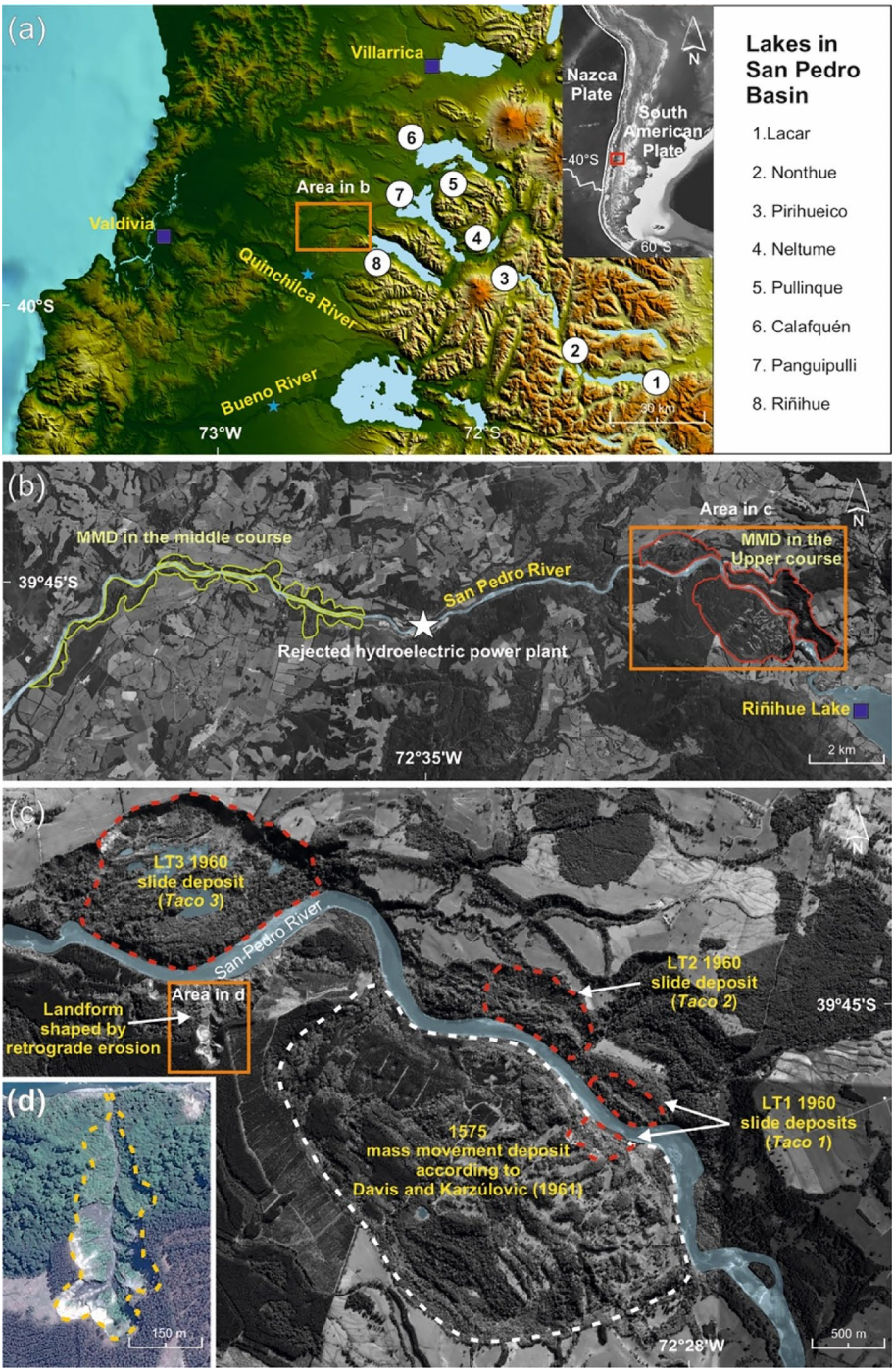

Fig. 2 **a** Study area and the SPR basin. **b** and **c** Landslides in the upper and middle course of the SPR. **d** Gully was shaped by retrograde erosion from improper land use in the early 2000s

2 Study area

The SPR originates near the foothills of the Andes and connects the Riñihue Lake with the Pacific Ocean. Its hydrographic catchment is composed by seven other lakes, five in Chilean territory and two in Argentina, with an overall area of ~ 450 km^2 (Fig. 2a). The interconnected system of lakes has a pluvio-nival regime, which naturally regulates the river. This makes that a large part of the sediment load transported from the upper catchment is deposited on the bottom of the lakes. For this reason, the SPR has a very low suspended sediment load (Habit and Parra 2012). Given the extensive hydraulic catchment and its precipitation regime (~ 2200 mm/yr), its damming could lead to a rapid accumulation of a vast amount of water, potentially leading to catastrophic outburst floods that threaten the ~ 160,000 people living downstream.

Regarding its seismotectonic setting, the SPR is located in the south-central part of the seismically active subduction zone of Chile (Fig. 1). Along this zone, the Nazca oceanic plate subducts beneath the continental South America plate at a convergence rate of ~ 65–70 mm/year (Angermann et al. 1999). According to the historical record, the 1,000 km long southern segment of this subduction zone has generated at least four major megathrust earthquakes (M8+) in the past 500 years (e.g., Lomnitz 2004). The sequence includes the 1960 event (M9.2–9.6), the largest instrumentally recorded worldwide (Kanamori and Cipar 1974), and other great earthquakes in 1575, 1737, 1837 of unknown magnitudes but most likely greater than 8 (Lomnitz 1970; Cisternas et al. 2005; Moernaut et al. 2014; Ruiz and Madariaga 2018; Matos-Llavona et al. 2022). Historical documents (Cisternas et al. 2017a) and sedimentary records at the coast (Cisternas et al. 2017b) and within inland lakes (Moernaut et al. 2014; Wils et al. 2020) indicate that the 1575 earthquake likely rivaled the 1960 earthquake in terms of magnitude and rupture extent. The smaller 1737 and 1837 earthquakes were likely limited to the northern and southern two-thirds of the 1960 rupture area (1,000 km long), respectively (Fig. 1b) (Cisternas et al. 2017a). Besides these very large events, the seismic catalogs show 26 poorly constrained events since 1570 with magnitudes apparently over 7 (white circles in Fig. 1a), which yield an average of 6.5 events per century in this area. The last of these was the instrumentally recorded M7.6 2016 Melinka earthquake, which ruptured a small, deep patch on the megathrust between latitudes 43 and 43.5° S (Moreno et al. 2018) (orange line in Fig. 1c).

The SPR is also exposed to intraplate earthquakes that occur either deep within the Nazca plate (brown line in Fig. 1c) or shallowly within the South America plate (green line in Fig. 1c). An important example of the latter source is the Liquiñe-Ofqui strike-slip fault. This fault, which runs only tens of kilometers east of the SPR, hosted the M6.2 Aysén earthquake discussed in the introduction. Although there is no instrumental record of great intraplate earthquakes within the downgoing slab in our study area, these types of earthquakes have been widely reported further north and have been accompanied by strong yet localized earthquake shaking. The most remarkable example is the M ~ 7.8 1939 Chillan intermediate-depth earthquake (Beck et al. 1998; Ruiz and Madariaga 2018) which caused ~ 20,000 deaths (1939 event in Fig. 1a, b).

3 Methods

We study the landslide deposits of the 1960 and earlier south Chile earthquakes present in the upper course of the SPR by combining multiple sources of information. These include field observations, satellite and LiDAR imagery, and previously published and newly found historical accounts. In this section, we detail each of these and explain how these are combined to achieve the overarching goal.

3.1 Characterization of landslide deposits

The geomorphologic and sedimentologic features of the main landslide deposits at the upper course of the SPR were characterized by field observations made in January 2014 and 2015, and satellite imagery from 2016. On the field, we reviewed the state of different landslide deposits on both banks of the upper course of the SPR, including *Tacos* 1, 2, and 3, and other ancient landslide deposits (e.g., see Figs. 3, 4, 5 and 6).

For the remote sensing analysis, we obtain satellite images (1:10,000 and 1:5,000) of Google Earth software (in Figs. 2b, c, d, and 5a) and aerial photographs (1:10,000) of the Chilean Air Force flight made in 1961 (in Figs. 4a and 5c). These images and photographs were processed with the GIS ArcMap of ArcGIS 10.3 and ERDAS Imagine 2014 software.

The studies by Davis and Karzulovic (1961) and Rodríguez et al. (1999) were used for the geological and sedimentological description. To improve the knowledge about the landslides deposit, we elaborated a geomorphological map for our study area on ArcMap (Fig. 3). We used the geomorphologic study of Laugenie (1982) as a reference due to include the first detailed geomorphic description of the study area, which was complemented by using satellite images and field observations to improve the accuracy of the analysis.

Also, we studied the evolution of the larger slide deposit generated by the 1960 earthquake using two topographic profiles obtained by Davis and Karzulovic (1961). Its location was georeferenced using ArcMap and was compared with two profiles from a cloud of LIDAR points (2–3 points/m^2) obtained in 2009 (Fig. 4). The LIDAR information was processed with ArcMap using the LAS Dataset tool, allowing the removal of the dense vegetation from the surface of the landslide deposits present on the river valley of the SPR. With the information resulting from this process (LAS data), a raster image was created and used to elaborate the profiles shown in Figs. 4c and 5b, also using ArcMap. A digital terrain model (DTM) of 50 cm resolution, visible in Fig. 4b, was elaborated in ERDAS imagine 2014. The same DTM was used as a basis to develop the geomorphological map (Fig. 3).

3.2 Erosion rate of LT3 (*Taco 3*) scarp

We studied the erosion rate along the largest slide deposit generated by the 1960 earthquake, hereafter referred to as LT3. The erosion rate (E), defined as the annual amount of eroded material from the scarp that forms part of LT3, was estimated from:

$$E = \frac{M}{t} \tag{1}$$

where M (kg) is the amount of mass removed from the scarp and t (years) is the elapsed time. The period considered is 50 years, between 1960 and 2010. The input for this calculation was obtained from the two topographic profiles (A–A' and B–B', Fig. 4b) reported in

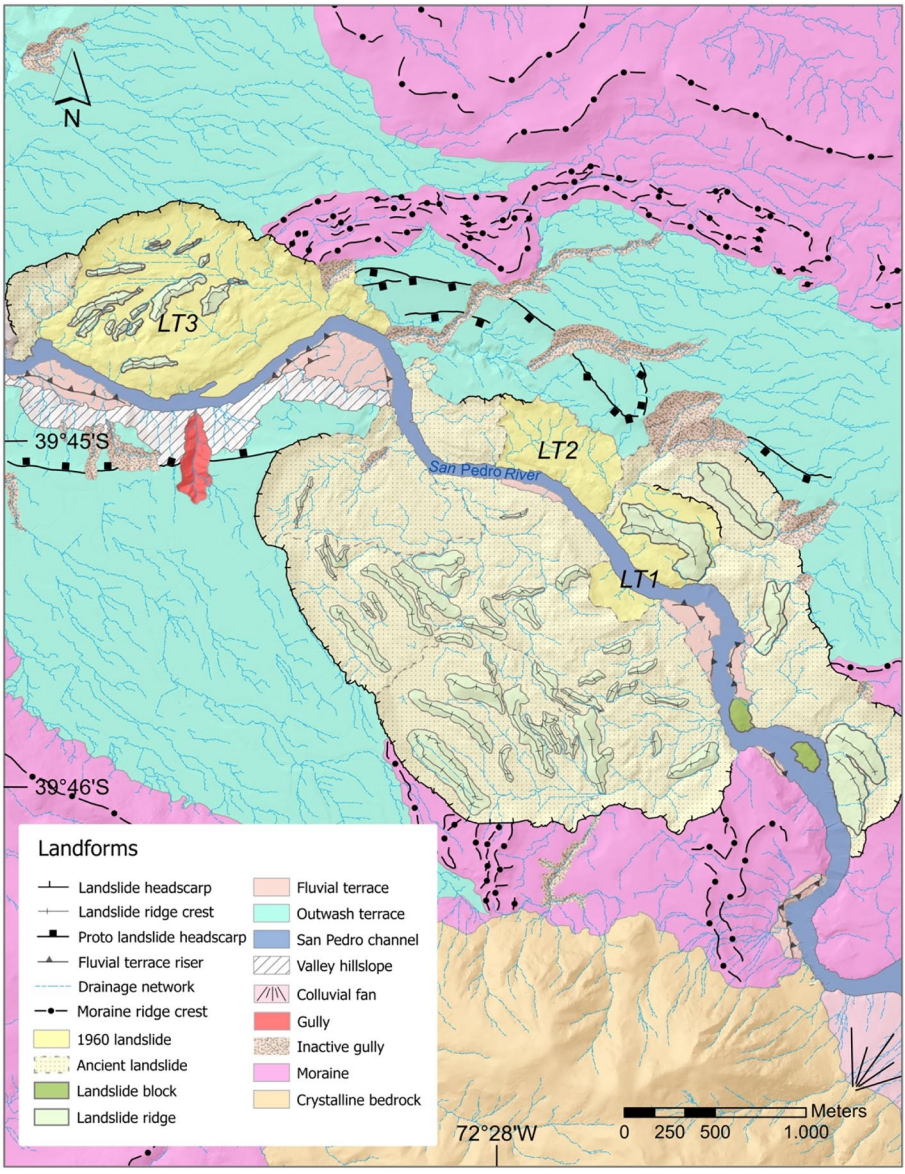

Fig. 3 Geomorphological map based on Laugenie (1982) and own observations

the paper of Davis and Karzulovic (1961), and from LIDAR information processed in the GIS. Only the surface of the escarpment was considered and not the deposit in the toe. As a result, two E values were obtained, one for each topographic profile and associated scarp.

Our calculations also considered depth-dependent changes in the density of the deposits that formed the scarp. We use the densities present in Noguera and Garcés (1991), obtained by drillings executed on the outwash terrace where LT3 originated, close to the main scarp. The density of sediments changes significantly at 16 m depth.

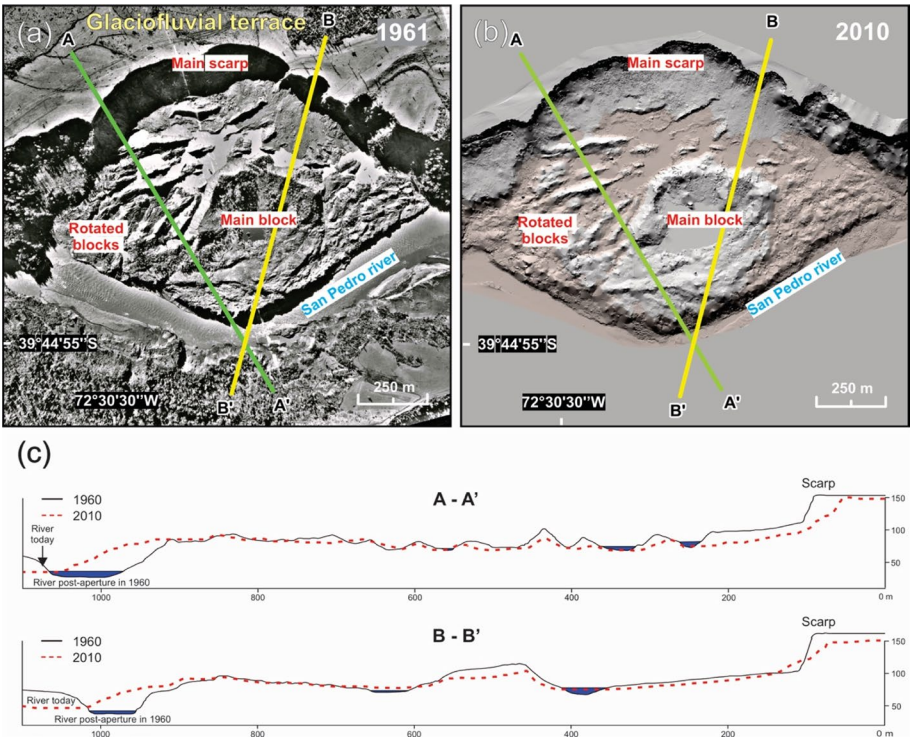

Fig. 4 **a** LT3 main geomorphological features in aerial photography (Chilean Air Force, 1961) and **b** 2010 LT3 DTM LIDAR-based information. **c** Topographic profiles (profiles lines in A and B) obtained from Davis and Karzulovic (1961) (A-A'/B-B') compared to profiles obtained from LIDAR-based information

Therefore, using the Noguera and Garcés (1991) data, a density of $\rho = 1{,}780$ kg/m^3 and $\rho = 2{,}380$ kg/m^3 was considered for the upper part and the rest of the scarp, respectively. Finally, the mass removed from the scarp was obtained by computing the weighted average between the eroded volume and its respective density.

3.3 Historic archives

We complement previously published with newly found historical records to improve our knowledge about the landslide deposits that dammed the SPR in 1575. Newly found records came from the *Archivo Nacional* in Santiago, Chile. This archive contains manuscripts generated in the Governorships and Captaincies belonging to the Viceroyalty of Peru of the Spanish Empire (including Chile, which was a Captaincy) and which were directed toward authorities who lived in America as the Viceroy. This is the most important historical archive in Chile and contains records issued to local authorities. Here, we found three unpublished manuscripts that refer to the landslide that dammed the SPR in 1575, which we describe in Table 1 and in the supplementary material (Texts S1, S2, and S3).

4 Results

4.1 Geomorphological and geological settings

The local geomorphological setting of the upper course of the SPR is a relevant factor in explaining the presence of landslide deposits triggered by earthquakes. The river valley of its middle and upper courses shows morphological features related to multiple landslide deposits similar to those triggered by the 1960 earthquake, which cover an area of ~ 10 km^2 (Fig. 2b). These features are clearly identifiable in satellite images due to their morphology and because they exhibit well-defined headscarps. The latter are coalescent, such as some existing landslides in the upper course. Also, the landslide deposits in the middle course show a smoother surface, suggesting that the deposits are older than the upper course landslide deposits. Also, these deposits can determine the sinuosity of the river. Interestingly, these phenomena have not been recorded either geomorphologically or historically in neighboring basins of tributary rivers, despite their similar seismic exposure and climatic conditions (e.g., Quinchilca and Bueno rivers, Fig. 2a).

The landforms associated with glacial processes correspond to different types of moraines related to the position of the glacier front. These moraines are arcuate-shaped, characterized by an irregular surface, and are not in direct contact with the course of the SPR (Fig. 3). Closer to the river is the outwash terrace, a relatively flat relief at ~ 260 m.a.s.l. from where all landslides are generated (Fig. 3). The high susceptibility to faulting and the high erosivity evidenced by the multiple landslide deposits and by the multiple gullies (inactive and active) present in the upper course of the SPR (see Fig. 3) may be due to the type of deposits that conform landforms such as the outwash terrace.

The local stratigraphy at the upper river course is formed by deposits originating in glacio-lacustrine and glacio-fluvial environments, inherited from the last glacial/interglacial periods and the current postglacial. Moraine deposits intercalate with glacio-fluvial sediments, and deformed laminated silts and clays were observed by Davis and Karzulovic (1961) in the scarp (on the outwash terrace). These deposits of lacustrine origin, according to Davis and Karzulovic (1961), were the basal layers of the slide that generated LT3 (~ 60 m, Figure S1b). Laboratory tests on sediments from two drillings suggest that some deposits liquefied during the 1960 earthquake. These correspond to perturbed silty strata with some sands and gravels (Noguera and Garcés, 1991). This type of sediment combination (silt, sand, and gravel) can be seen in the scarp, between ~ 19 and ~ 29 m deep (Figure S1b).

4.2 Characteristics and evolution of LT3

4.2.1 The sliding process

The deposit of LT3 was generated by a multirotational slide (Hauser 2000). At the time of its formation, the slide generated an average scarp height of 40 m. The slide deposit was made up of a debris apron, a series of failed and rotated blocks, a large unitary block, folds, and a terminal zone or toe corresponding to the propagation front that went toward the SPR (Fig. 4a). The toe and the unitary block were the sections of the slide that dammed the riverbed. The river eroded the toe after the work carried out for the controlled opening of the *Tacos*, modifying the original course.

Fig. 5 **a** and **b** Landslide deposit profiles in the SPR upper course. Elevations are in meters above sea level (m.a.s.l.). **c** Scarps of slide deposit that generated LT1 and evidence of reactivation of scarps of ancient MM by the 1960 earthquake (Aerial photography from Chilean Air Force, 1961)

In the first months after the slide, critical erosive processes, and deposits such as pediments, cones, fans, deltas, drainage systems, and block rounding were observed (Davis and Karzulovic 1961). This was accelerated by the typically abundant precipitation in south Chilean winter, the initial absence of vegetation, and many water springs that arose from the different porous sediments of the escarpment wall, discharging water toward the slide deposit.

4.2.2 The evolution of LT3

In 50 years (1960–2010), the LT3 landform underwent important changes in the main scarp (Fig. 4c) since it shows a notable setback and a decrease in its slope gradient (see Sect. 4.2.3). The other main structures of the landslide deposit, such as the rotated blocks and the unit block, have been preserved without major changes. Only a smoothing and lowering of its slopes are observed. Some lagoons formed in 1960 persist, while the others have been filled with sediments and/or drained. Moreover, vegetation coverage has increased in height and density. According to what is revealed by comparison made with LIDAR information, the bed of the SPR is displaced toward the south for about 70 m (Fig. 4c), possibly caused by a lateral displacement of the slide deposit. If this phenomenon occurred, in conjunction with the dams formation, it indicates that the upper course of the SPR undergoes significant modifications in its shape and axis due to earthquake-triggered landslides and the post-depositional mobility of landslide deposits.

4.2.3 Scarp retreat

The scarp of the B–B' profile has a higher erosive rate than the scarp of A–A' (Fig. 4c). The A–A' scarp presents an average erosion rate of 39,000 kg/year per linear meter of the scarp, while the B–B' scarp averages a rate of 58,000 kg/year. This erosive rate is also reflected in the slope changes experienced by the escarpment: from 71° to 43° for A–A', and from 75° to 37° for B–B'. It should be considered that the escarpment of the B–B' profile had a greater height (10 m) and slightly steeper initial gradient.

According to descriptions of Davis and Karzulovic (1961), it can be inferred that the erosion index in 1960 was much higher than the averages described above because, at present, the same erosive phenomena described by these authors are not observed (see Sect. 4.2.1). The visible difference between initial and current erosion levels hampers the morphologic dating of the landslide deposits in the study area due to more homogeneous value being needed in a scarp formed at the same time or event. Additionally, some escarpments can be reactivated and/or accelerate their erosive processes with the occurrence of earthquakes (see Sect. 4.4.1).

4.3 Historical landslide damming of the SPR

4.3.1 Background of the landslides triggered by the 1575 and 1960 earthquakes

The SPR has been dammed at least twice since written history started in Chile in 1541. On both occasions, the trigger was strong shaking caused by the 1575 and 1960 earthquakes.

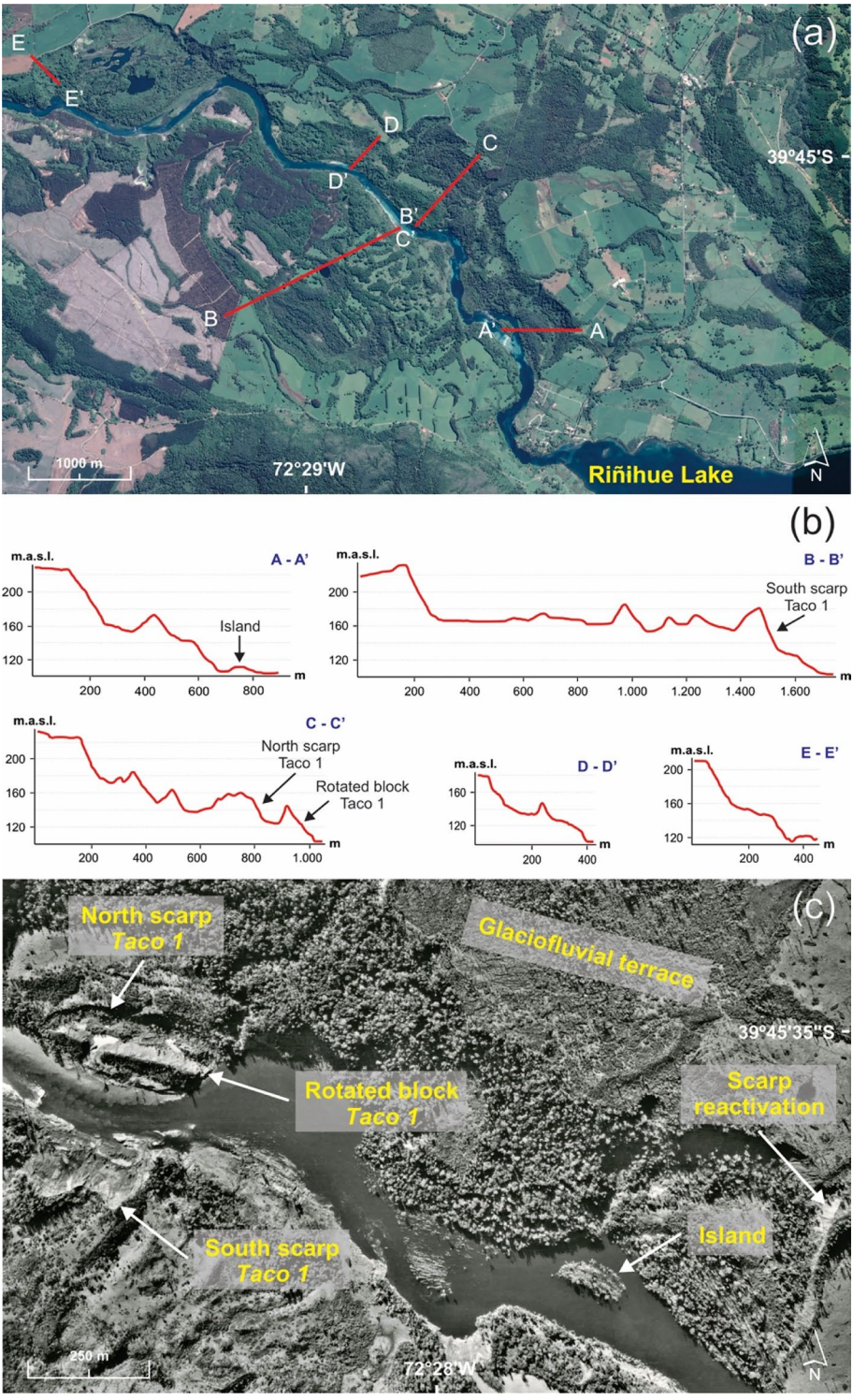
(a)
E
E'
D
D'
C
C'
B'
B
A'
A
39°45'S
1000 m
72°29'W
Riñihue Lake
N
(b)
m.a.s.l.
A - A'
Island
B - B'
South scarp
Taco 1
C - C'
North scarp
Taco 1
Rotated block
Taco 1
D - D'
E - E'
m
(c)
North scarp
Taco 1
Glaciofluvial terrace
39°45'35"S
Rotated block
Taco 1
Scarp
reactivation
Island
South scarp
Taco 1
250 m
72°28'W
N

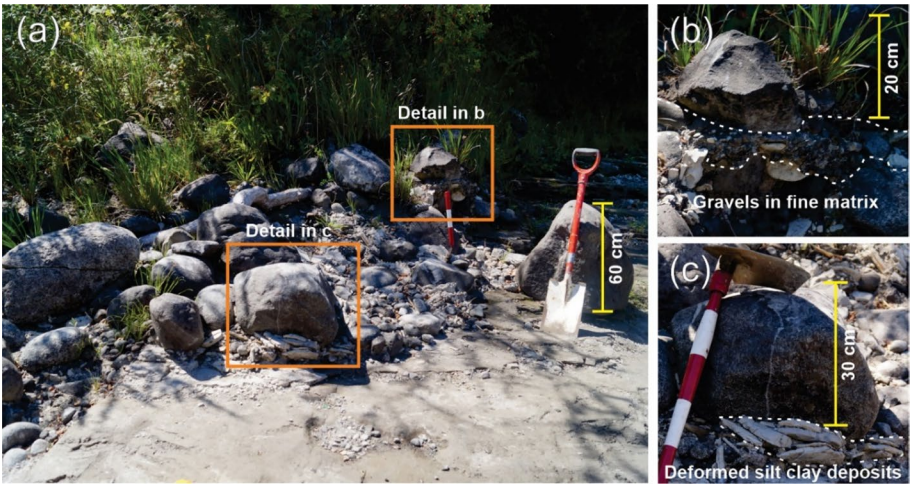

Fig. 6 Deposits in an island in the upper course of the SPR suggest that it was formed by an ancient landslide that dammed the river

Although multiple landslides were reported for the 1960 earthquake at different locations in south-central Chile (Weischet 1963; Wright and Mella 1963), those in the SPR reached public notoriety due to their threat to the ~ 60,000 inhabitants downstream. Three slides dammed the river. The volumes of sediments removed by these slides were 30×10^6, 6×10^6, and 2×10^6 m^3 (Davis and Karzulovic 1961). Due to the intervention of the State of Chile (National Electric Company) and the heroic effort of hundreds of locals, the dams were opened in a controlled manner through the construction of ditches to channel the water. All these events, given the proximity to Riñihue Lake, led to locals calling this historic event *Riñihuazo*.

In contrast, due to the 1575 earthquake, the population living downstream was severely affected. The historical chronicles compiled by Montessus de Ballore (1912) and Cisternas et al. (2005) describe that the formation of the natural dam caused water accumulation for nearly 5 months, collapsing catastrophically with the resulting outburst flood, taking the lives of 800 to 1,200 aborigines, according to data estimated by colonial authorities and witnesses. However, none of the authors of the chronicles compiled by Montessus de Ballore described the landslide that blocked the river. Based on morphological features, Davis and Karzulovic (1961) proposed that one of the deposits present in the upper course of the SPR (three times bigger than LT3) corresponds to the landslide that occurred in 1575 (Fig. 2c). However, the historical evidence presented below does not support the source proposed by Davis and Karzulovic (1961).

4.3.2 Historical evidence of the 1575 landslide

Our bibliographic and archive search resulted in nine historical documents that refer to the deposit of the 1575 event (Table 1). Among these, one written by an anonymous author provides the only direct observations of the landslide deposit at the time when it was still damming the SPR. The report describes both its size and approximate location. Interestingly, both the size and location inferred from this first-hand account do not coincide with those suggested by Davis and Karzulovic (1961) based on morphological appearances. The

Table 1 Historical data obtained from settlers of the 1575 landslide (*L*)

Type of historical source	Author	Place of origin	Date	Eyewitness?	N° of L described	Location	Size of L (m^3)	Lake level rise (m)	Source
Letter	Pedro Feyjó	Valdivia	12/28/1575	No	1	Outflow of Riñihue Lake	–	–	In Cisternas et al. 2005
Letter	Cabildo de la Imperial	La Imperial	01/08/1576	No	2	Outflow of Riñihue Lake	–	–	In Cisternas et al. 2005
Letter	Martín Ruiz de Gamboa	Concepción	02/12/1576	No	–	Outflow of Riñihue Lake	–	–	In Cisternas et al. 2005
Letter	Francisco de Gálvez	Santiago	02/21/1576	No	2	–	–	–	Unpublished. See in supplementary Text S1
Relation	Anonymous	–	Between December 1575 and April 1576	No	–	Outflow of Riñihue Lake	–	~70	in Silgado 1985
Letter	Antonio Carreño	Santiago	08/10/1576	No	–	Outflow of Riñihue Lake	–	~80	Unpublished. See in supplementary Text S2
Relation	Antonio Carreño	Santiago	10/10/1576	No	–	Outflow of Riñihue Lake	–	~80	Unpublished. See in supplementary Text S3
Chronicle	Pedro Mariño de Lobera	Santiago	–	No	1	Outflow of Riñihue Lake	–	–	In Montessus de Ballore 1912; in Cisternas et al. 2005
Relation	Anonymous	Arauco Province	Between 1576 and 1598	Yes	1	Outflow of Riñihue Lake	~1×10^6 *	~50	In Silgado 1985

*1×1 quarter pace and 30 "*estados*" high

landslide deposit suggested by these authors is located 2 km away from the outflow of Riñihue Lake (Fig. 2c). However, the eyewitness reported a location right at the outflow of Riñihue Lake and had an associated volume of ~ 1.2×10^6 m^3 and an area of ~ 15,000 m^2 (according to the official measurement unit used in those years (e.g., De Ramón and Larraín, 1979)), which is about half the volume of LT1 and ~ 200 times smaller than the landslide proposed by Davis and Karzulovic (1961). Seven other secondary sources support the location reported by the eyewitness (Table 1). Although, as a result of our exhaustive search in the historical archives, no other witness to the landslide was found, it can be verified that the knowledge of the people of that time indicated that the location of the event was close to the Riñihue Lake outflow and that the water level rose several tens of meters.

4.4 Ancient landslide deposits as evidence of recurrent earthquakes

4.4.1 Characteristics of ancient landslide deposits in the SPR upper course

Damming of the SPR by landslides is reported twice in the historical records. This situation raises the possibility that prehistoric earthquakes also dammed the SPR. Morphological similarities between ancient deposits at the SPR and those associated with the 1960 earthquake support this possibility.

Traces of the ancient deposits, potentially associated with earthquake-induced landslides, are shown in Fig. 5. Among their main characteristics, they feature escarpments of 20 m or more with slopes above 30° and exhibit a slide body that project into the river with one or more ridges. Two ancient landslide deposits (visualized in B–B' and C–C' profiles, Fig. 5b) were modified by the 1960 earthquake because the slides that generated the LT1 were formed on a section of these (Fig. 5c). In contrast, the deposit of the LT2 represented in the D–D' profile (Fig. 5b) originated entirely in the 1960 earthquake. The deposits represented by the A–A' and E–E' profiles in Fig. 5b have morphological characteristics similar to the other deposits previously described and presented reactivations of their scarps during the 1960 earthquake, which can be observed for the E–E' profile in Fig. 5b. All the elements described above suggest that although some deposits may have been formed in a single event, others were caused by remobilizing preexisting landslide deposits.

This data suggests that a landslide deposit can be formed by one or more events generated at different times. If the historical records (size and location) are considered, the proposal of Davis and Karzulovic (1961) for the 1575 landslide becomes even more debatable because the proposed deposit can be made up of more than two events. The deposit represented by A–A' profile in Fig. 5b is closer to the Riñihue Lake outflow, and its section bordering the river could be considered a possible candidate for the 1575 river-damming landslide deposit. This hypothesis considers the morphology, the size, and the location revealed by the historical evidence, in addition to the presence of an island as a typical characteristic of landslide deposits in this locality (see Sect. 4.4.2 and Fig. 6). Such a hypothesis must be approved or rejected in future works, including detailed geomorphological and geological analyses (e.g., geological-geotechnical analyses) of the island and the adjacent landslide deposit.

4.4.2 River islands as evidence of ancient landslides?

The islands along the upper and middle course of the SPR may have been formed from ancient landslides as well. Similar islands formed by landslides have also been observed by

Hewitt (1998) in the upper course of the Indus River in Pakistan. One of the islands in the upper course of the SPR was investigated in the field and had characteristics that suggest a colluvial and non-fluvial origin. Its location (facing an ancient landslide deposit), size, geological composition, and low sediment load of the river support this proposal (island in Fig. 6b and 6c).

The aforementioned island currently has an area of ~ 1.4 ha, a height of ~ 4 m above the average river water level, and shows dense vegetation on its surface. The island existed before the 1960 event (Fig. 5c), so it resisted, at least partially, the water-level increase and controlled river discharge during the *Riñihuazo*. Its presence is remarkable considering that the upper course of the SPR is devoid of sediment load as Riñihue Lake and the other lakes upstream act as sediment traps. This situation, combined with other factors such as slope (1%) and average flow (~ 400 m^3/s) (Habit and Parra 2012), determines the presence of bedforms, such as middle and lateral banks. The island deposits consist of outwash terrace material and morainic deposits, similar to landslide deposits alongside the SPR. The previous is supported by poor sorting and the existence of rounded to sub-rounded blocks in a matrix of fine sediments (silts and clays) and gravels (Fig. 6b and 6c) materials that are observable on the LT3 escarpment (Figure S1b) and in its deposits (Davis and Karzulovic 1961). Even clayey silt sediments are indicated by authors such as Noguera and Garcés (1991) and Zúñiga Álvarez (2019) as highly sensitive to failure when saturated.

Although it is a hypothesis that must be tested in future studies, collectively, these observations suggest that this island was part of an ancient landslide that could have dammed the SPR. Also, it indicates that the other islands located further downstream, which face ancient landslide deposits, are landslide vestiges rather than fluvial deposits.

5 Discussion

Studying past landslide events provides essential knowledge to prevent future disasters (Rabby et al. 2023). Thus, scientific work focused on improving the inventory of earthquake-triggered landslide deposits (e.g., spatiotemporal distribution), characterizing their forcing mechanisms (e.g., terrain parameters), such as its evolution and the occurrence susceptibility, can provide critical information for the hazard assessment in areas affected by these phenomena (Harp et al. 2011; Pokharel et al. 2021; Bhuyan et al. 2023; Fan et al. 2023).

As reviewed in the previous sections, the 1575 and 1960 earthquakes must have generated sufficient local seismic intensities to trigger a landslide capable of damming the upper course of the SPR. Compared with the other earthquakes in the historical sequence, stronger and more prolonged shaking from these events is consistent with the turbidite record and soft-sediment deformation structures in Riñihue Lake and other nearby lakes (Moernaut et al. 2014; Molenaar et al. 2022). Based on the similar thickness and extensive distribution of the 1575 and 1960 turbidite deposits, Moernaut et al. (2014) inferred seismic intensities of about MMI VII½ for the 1575 earthquake in Riñihue Lake. On the other hand, the lack of conspicuous landslide evidence associated with the 1737 and 1837 earthquakes agrees with the smaller inferred seismic intensities (about VI½) based on the modest size of turbidites in the Riñihue Lake sedimentary record (Moernaut et al. 2014). While it might seem tempting to link these shaking inferences with earthquake source characteristics, such as similarities or differences in the slip distribution of the historical seismic sequence, other factors, in addition to the seismic intensities reached, also contribute

to landslide triggering (e.g., slope) (Serey et al. 2019). Serey et al. (2019) highlight these complexities in their study of landslides caused by the 2010 earthquake, which occurred just north of our research area.

Therefore, from a risk assessment viewpoint, the following question arises: What are the present factors that influence the triggering of landslides in the upper SPR, and what are the scenarios capable of triggering a landslide in this zone? Although addressing these questions is challenging, what we have learned from studying past landslide deposits and knowledge derived from recent events helped us make some reasonable speculations. If we assume that geological and seismological boundary conditions have been relatively constant in the past few millennia, then it is reasonable to consider climate seasonality, transient climatological events (e.g., ENSO events), geomorphological evolution, and land use as factors that affect the generation, quantity, and dimensions of landslides. Among the above, land use is one of the factors that most influence the generation of landslides, directly or indirectly, when combined with other factors (Pacheco Quevedo et al. 2023). As was recently demonstrated by the September 2018 Mw 7.5 earthquake in Sulawesi, Indonesia, improper land-use management combined with strong shaking events can cause catastrophic consequences for the population due to landslides (Bradley et al. 2019; Watkinson and Hall 2019).

Moreover, landslides can be generated due to improper land use alone, without earthquake triggering, in valleys with similar geologic and geomorphic setting to the SPR. This was the case of the landslide that dammed the Colca River Valley, Peru, in June 2020. The Colca River Valley, which exhibits multiple landslide deposits on its surface, have tectonic (e.g., subduction and crustal earthquakes) and geological (e.g., lacustrine sediments composed of sand and laminated silts/clays) conditions that favor its generation (Bontemps et al. 2020; Gaidzik et al. 2020). Although many of these landslides may be related to earthquakes (Gaidzik et al. 2020), in 2020 a ~ 14×10^6 m^3 landslide was generated without an earthquake, and its origin is attributed to the strata saturation conditions associated with land use (e.g., type of irrigation) and rainfall (INGEMMET 2020). In the study area, 40,000 m^2 of landforms of erosive origin can be observed, specifically, a retrograde erosion landform shaped by improper land use (Fig. 2c and 2d), which shows that geological and anthropic conditions can initiate mass movement processes.

At the SPR, the influence of seasonality and land use can be evaluated because although Moernaut et al. (2014) assign similar local seismic intensities between the earthquakes of 1575 and 1960, the historical evidence reveals variations regarding the quantity and size of the landslides that they generated. Although in our search in the historical archives, we found new records that mentioned the landslide of 1575, we did not find a record of someone who had witnessed the landslide, leaving only the eyewitness published by Silgado (1985) (see Sect. 4.3.2). Assuming that the testimony of the only known eyewitness is credible, the 1575 earthquake generated a single landslide deposit that reached an approximate dimension of about 1.2×10^6 m^3, equivalent to half the size of the slide generated by LT1 and 1/30 of LT3.

According to the Chilean General Direction for Water, annual rainfall is ~ 2200 mm, with peaks occurring in autumn and winter (Riñihue Lake station, General Direction for Water 2019). The 1960 earthquake occurred in autumn on May 22, and the annual rainfall accumulated up to that date was 580 mm (Chilean Meteorological Direction 2019). This amount of accumulated rainfall favored a saturation of the fine, sensitive strata, being decisive for the generation of slides on nearly horizontal strata (Noguera and Garcés, 1991). The above is supported by the work of Zúñiga Álvarez (2019), which establishes that the clayey silt sediments of the outwash terrace become highly sensitive to

failure when saturated and even require lower local intensities than those generated by the 1960 earthquake to fail. In contrast, the event of 1575 occurred on December 16, that is, entering the summer so the strata may have been saturated to a much smaller degree than in the case of the 1960 event. Possibly, these seasonal variations partly explain the differences in quantity and size of deposits generated by the 1575 and 1960 events.

In 1575, there was no evidence of settlements or significant extractive activities in the upper course of the SPR, neither Spanish nor indigenous, so the forest vegetation was practically pristine (Solari et al. 2011). In general, less vegetation cover on non-rocky slopes influences the saturation of the strata and the water table, making them more susceptible to failure (Wu and Sidle 1995), whereas for 1960, the aerial photographs show grasslands with subdivisions and soil with scarce arboreal vegetation (agricultural use), as seen in the outwash terrace where LT3 was formed (Fig. 4a). Therefore, it is reasonable to think that given the same external factors, the slopes and surfaces in 1575 could have been less susceptible to failure than in 1960 due to the greater vegetational coverage and the better condition of the soils or substratum, which allowed for less infiltration and saturation of pores in the strata. Additionally, the river flow growth due to the accumulated rainfall in 1960 may be a factor that preconditions landslide generation due to river undercutting of the toe of landslide deposits and other landforms of the river valley.

These differences suggest that the landslides originated in 1960 may not have occurred in such quantity and magnitude if the earthquake had occurred in a drier season and/or with less human intervention, as in 1575. In any case, the historical landslides and river damming occurred despite differences in season or land use, so these aspects may be less critical than the seismic or geological factors, especially knowing the faulting susceptibility of some strata of the outwash terrace from where all landslides occur.

Future risk assessments concerning the SPR should acknowledge that the potential for its damming is not solely reliant on the occurrence of a giant earthquake, as previously thought. Smaller and more frequent earthquakes accompanied by locally intense shaking, improper land use, river flooding that erodes part of the toe of a landslide deposit, or a combination of the above processes, can cause river-damming landslides. Likewise, it must be considered that not only a large landslide such as LT3 is necessary to dam the river. Just one of the LT1 sizes is enough to dam the SPR, as it happened in 1960 or, if the historical testimony is true, as in 1575, because the capacity of damming depends mainly on the size of the landslide and the relative size of the valley.

Finally, it must be taken into account that the next landslide that dams the SPR will probably occur from the outwash terrace or a landslide deposit. The first may occur because all the landslides have been generated from the terrace, it was reactivated during the 1960 earthquake (see Fig. 5c), and even a gully has formed due to improper management (Figs. 2d and 3), which shows its sensitivity to failure. Additionally, Davis and Karzulovic, using aerial photographs prior to 1960, establish that the origin of LT3 came from the terrace that was apparently presenting settlement and creep phenomena (Davis and Karzulovic 1961:99). Although, in this study, an apparent movement of LT3 is registered (see Fig. 4c), this must be verified with methods that allow reviewing slow terrain changes recent (horizontals and verticals) with greater precision, such as InSAR or ideally with comparisons with LiDAR information. The second, that is, the formation of new landslides from landslide deposits, may happen because it also occurred during the 1960 earthquake (see Sect. 4.4.1). This is expected in recently formed sediment deposits, such as those from the 1960s, which have not been completely consolidated and, therefore, can fail more easily. Any change in the slope, either artificial (e.g., slope cuts for constructions) or

natural (e.g., an increase in river flow due to extreme events), could lead to faulting from these landslide deposits.

6 Conclusions

The evidence offered in this work shows how the upper course of the SPR is a complex geomorphic system and, from the geomorphological, geological, and hazard perspectives, represents a singularity. Its particularities can be summarized in: a series of landslide footprints that mark the valley and do not show other neighboring basins, the historical landslides that have dammed the river, and its sensitivity to past phenomena, such as earthquakes and recent ones, related to an inappropriate land use that is reflected in the formation of gullies. The different approaches used here, such as the analysis of historical records, the review of landslide deposits using different remote sensing tools (aerial photographs, satellite images, LiDAR information), and the analysis of the evolution geomorphology of the deposit of the largest landslide generated by the 1960 earthquake (LT3), allow us to support the findings that define its singularity.

Our results have important implications for risk assessment in the SPR. Future risk assessments, especially associated with recent or ongoing projects in the river valley (e.g., rejected hydroelectric power plant, see Fig. 2b), should consider multiple factors influencing river-damming hazards. These factors include the geological conditions of the valley, land use, and shaking from smaller, frequent earthquakes. Additionally, these risk assessments must consider the historical evidence showing that a relatively small landslide can dam the SPR, such as the LT1 of 1960 and the 1575 earthquake-triggered landslide deposit.

Supplementary Information The online version contains supplementary material available at https://doi.org/10.1007/s11069-024-06474-8.

Acknowledgements CAC acknowledges the support of the Doctoral program of the Institute of Geography of the Pontificia Universidad Católica de Chile. MC and DM acknowledge the support of the Iniciativa Científica Milenio (ICM) through Grant NºNC160025 and the Chilean National Fund for Development of Science and Technology (FONDECYT) Nº1231735. JM acknowledges the support of the Austrian Science Fund (FWF), project NºP34504. Special thanks to Marco Cisternas for his support and valuable ideas and Fernando Torrejón for his collaboration in the search for unpublished historical information and his references to information already published.

Author contributions CAC, MC, DM, and JM led the preparation of the manuscript and conceptualized the research. CAC, DM, and JM collected field data and assisted in logistics. DM obtained the main source of funding for this project. CAC and MC analyzed and contextualized the historical information about the earthquakes. CAC, DM, and JM performed the landslide analysis. CAC and CA processed the GIS information, including the LiDAR data and elaborated the geomorphological map. CAC and FG collected information and calculated the erosion rate of the LT3 scarp. All authors contributed to the review and editing of the final manuscript.

Funding This work was supported by the National Agency for Research and Development of Chile (ANID) through the following programs: Millennium Scientific Initiative (ICM), Grant/Award Number: NC160025; Chilean National Fund for Development of Science and Technology (FONDECYT), Grant/Award Number: 1231735; and Doctoral support program Grant/Award Number: 21201355. Austrian Science Fund (FWF), project number P34504.

Declarations

Conflict of interest The authors declare no conflict of interest.

References

Agurto H, Rietbrock A, Barrientos S, Bataille K, Legrand D (2012) Seismo-tectonic structure of the Aysén Region, Southern Chile, inferred from the 2007 Mw = 6.2 Aysén earthquake sequence. Geophys J Int 190(1):116–130. https://doi.org/10.1111/j.1365-246X.2012.05507.x

Alexander D (2012) Vulnerability to Landslides. In: Glade T, Anderson M, Crozier MJ (eds) Landslide hazard and risk. John Wiley & Sons Ltd, Hoboken, pp 175–198

Angermann D, Klotz J, Reigber C (1999) Space-geodetic estimation of the Nazca-South America Euler vector. Earth Planet Sci Lett 171(3):329–334

Antinao JL, Gosse J (2009) Large rockslides in the Southern Central Andes of Chile (32–34.5°S): tectonic control and significance for quaternary landscape evolution. Geomorphology 104(3):117–133. https://doi.org/10.1016/j.geomorph.2008.08.008

Astroza M, Ruiz S, Astroza R (2012) Damage assessment and seismic intensity analysis of the 2010 (M-w 8.8) Maule earthquake. Earthq Spectra. https://doi.org/10.1193/14000027

Astroza M, Lazo R (2010) Estudio de los daños de los terremotos del 21 y 22 de Mayo de 1960. Paper presented at the X Jornadas de Sismología e Ingeniería Antisismica, Santiago, Chile

Astroza M, Moya R, Sanhueza S (2002) Estudio comparativo de los efectos de los terremotos de Chillan de 1939 y de talca de 1928. Paper presented at the VIII Jornadas Chilenas de Sismología e Ingeniería Antisísmica, Valparaíso, Chile

Beck S, Barrientos S, Kausel E, Reyes M (1998) Source characteristics of historic earthquakes along the central Chile subduction askew et alzone. J S Am Earth Sci 11(2):115–129

Bhuyan K, Tanyaş H, Nava L, Puliero S, Meena SR, Floris M, Catani F (2023) Generating multi-temporal landslide inventories through a general deep transfer learning strategy using HR EO data. Sci Rep 13(1):162

Bontemps N, Lacroix P, Larose E, Jara J, Taipe E (2020) Rain and small earthquakes maintain a slow-moving landslide in a persistent critical state. Nat Commun 11(1):1–10

Bradley K, Mallick R, Andikagumi H, Hubbard J, Meilianda E, Switzer A, Benazir B (2019) Earthquake-triggered 2018 Palu valley landslides enabled by wet rice cultivation. Nat Geosci 12:1–5

Budimir MEA, Atkinson PM, Lewis HG (2015) Earthquake-and-landslide events are associated with more fatalities than earthquakes alone. Nat Hazards 72(2):895–914. https://doi.org/10.1007/s11069-014-1044-4

Cisternas M, Atwater BF, Torrejón F, Sawai Y, Machuca G, Lagos M, Kamataki T (2005) Predecessors of the giant 1960 Chile earthquake. Nature 437(7057):404

Cisternas M, Carvajal M, Wesson R, Ely LL, Gorigoitia N (2017a) Exploring the historical earthquakes preceding the giant 1960 Chile earthquake in a time-dependent seismogenic zone. Bull Seismol Soc Am 107(6):2664–2675. https://doi.org/10.1785/0120170103

Cisternas M, Garrett E, Wesson R, Dura T, Ely L (2017b) Unusual geologic evidence of coeval seismic shaking and tsunamis shows variability in earthquake size and recurrence in the area of the giant 1960 Chile earthquake. Mar Geol 385:101–113

Davis S, Karzulovic J (1961) Deslizamientos en el valle del río San Pedro provincia de Valdivia, Chile. Paper presented at the Anales de la Facultad de Ciencias Físicas y Matemáticas

Fan X, Scaringi G, Korup O, West AJ, van Westen CJ, Tanyas H, Huang R (2019) Earthquake-induced chains of geologic hazards: Patterns, mechanisms, and impacts. Rev Geophys 57:421–503

Fan X, Dufresne A, Subramanian SS, Strom A, Hermanns R, Stefanelli CT, Geertsema M (2020) The formation and impact of landslide dams–state of the art. Earth-Sci Rev 203:103116

Fan X, Liu B, Luo J, Pan K, Han S, Zhou Z (2023) Comparison of earthquake-induced shallow landslide susceptibility assessment based on two-category LR and KDE-MLR. Sci Rep 13(1):833

Gaidzik K, Żaba J, Ciesielczuk J (2020) Tectonic control on slow-moving Andean landslides in the Colca valley. Peru J Mt Sci 17(8):1807–1825

General Direction for Water (2019) Official Hydrometeorological and water quality information online. http://snia.dga.cl/BNAConsultas/reportes

Habit E, Parra O (2012) Fundamento y aproximación Metodológica del Estudio de peces del Río San Pedro. Gayana (concepción) 76:01–09

Harp EL, Keefer DK, Sato HP, Yagi H (2011) Landslide inventories: the essential part of seismic landslide hazard analyses. Eng Geol 122(1–2):9–21

Hauser A (2000) Remociones en masa en Chile (versión actualizada): Servicio Nacional de Geología y Minería

Hermanns RL, Valderrama Murillo PA, Fauqué LE, Penna IM, Sepúlveda SA, Moreiras SM, Zavala Carrión BL (2012) Landslides In the andes and the need to communicate on an Interandean level on landslide mapping and research. Rev De La Asoc Geol Argent 69(3):321–327

Hewitt K (1998) Catastrophic landslides and their effects on the Upper Indus streams, Karakoram Himalaya, northern Pakistan. Geomorphology 26(1–3):47–80
INGEMMET (2020) Deslizamiento de Achoma ocurrido el 18 de junio del 2020. Región Arequipa, provincia Caylloma, distrito Achoma. Instituto Geológico Minero y Metalúrgico, Dirección de Geología Ambiental y Riesgo, Perú, p 31
Kanamori H, Cipar J (1974) Focal process of the great Chilean earthquake May 22, 1960. Phys Earth Planet Inter 9(2):128–136
Keefer D (1984) Landslides caused by earthquakes. GSA Bull 95(4):406–421. https://doi.org/10.1130/0016-7606(1984)95<406:LCBE>2.0.CO;2
Keefer D, Larsen M (2007) Assessing landslide hazards. Science 316:1136–1138. https://doi.org/10.1126/science.1143308
Laugenie C (1982) La región des lacs, Chili meridional, recherches sur l'évolution géomorphologique d'un piémont glaciaire andin (Doctoral dissertation, Tesis de Doctorado de Estado, Universidad de Bordeaux III, Tomos 1 y 2, 822 p., Burdeos, Francia)
Lomnitz C (1970) Major earthquakes and tsunamis in Chile during the period 1535 to 1955. Geol Rundsch 59(3):938–960. https://doi.org/10.1007/bf02042278
Lomnitz C (2004) Major earthquakes of Chile: a historical survey, 1535–1960. Seismol Res Lett 75(3):368–378
Marc O, Hovius N, Meunier P, Uchida T, Hayashi S (2015) Transient changes of landslide rates after earthquakes. Geology 43(10):883–886
Matos-Llavona PI, Ely LL, MacInnes B, Dura T, Cisternas MA, Bourgeois J, Bruce D, DePaolis J, Dolcimascolo A, Horton BP, Melnick D (2022) The giant 1960 tsunami in the context of a 6000-year record of paleotsunamis and coastal evolution in south-central Chile. Earth Surf Proc Land 47(8):2062–2078
Meteorological Direction of Chile (2019) Climatological Yearbook. https://climatologia.meteochile.gob.cl/application/index/anuarios
Moernaut J, Van Daele MV, Heirman K, Fontijn K, Strasser M, Pino M, De Batist M (2014) Lacustrine turbidites as a tool for quantitative earthquake reconstruction: new evidence for a variable rupture mode in south central Chile. J Geophys Res Solid Earth 119(3):1607–1633. https://doi.org/10.1002/2013jb010738
Molenaar A, Van Daele M, Huang JJS, Strasser M, De Batist M, Pino M, Moernaut J (2022) Disentangling factors controlling earthquake-triggered soft-sediment deformation in lakes. Sediment Geol 438:106200
Montessus de Ballore F (1912) Historia sísmica de los Andes Meridionales al sur del paralelo XVI. Segunda parte. Imprenta Cervantes. Santiago
Moreno M, Melnick D, Rosenau M, Baez J, Klotz J, Oncken O, Hase H (2012) Toward understanding tectonic control on the Mw 8.8 2010 Maule Chile earthquake. Earth Planet Sci Lett 321:152–165
Moreno M, Li S, Melnick D, Bedford J, Baez J, Motagh M, Gutknecht B (2018) Chilean megathrust earthquake recurrence linked to frictional contrast at depth. Nat Geosci 11(4):285
National Seismological Center of Chile (2019) Great earthquakes in Chile. https://www.csn.uchile.cl/sismologia/grandes-terremotos-en-chile/
Noguera C, Garcés E (1991) Deslizamiento en el río San Pedro, analizado 30 años después. Paper presented at the Memorias, 9o Congreso Panamericano de Mecánica de Suelos e Ingeniería de Fundaciones, Viña del Mar, Chile
Pacheco Quevedo R, Velastegui-Montoya A, Montalván-Burbano N, Morante-Carballo F, Korup O, Daleles Rennó C (2023) Land use and land cover as a conditioning factor in landslide susceptibility: a literature review. Landslides 20:1–16
Pokharel B, Alvioli M, Lim S (2021) Assessment of earthquake-induced landslide inventories and susceptibility maps using slope unit-based logistic regression and geospatial statistics. Sci Rep 11(1):1–15
Rabby YW, Li Y, Hilafu H (2023) An objective absence data sampling method for landslide susceptibility mapping. Sci Rep 13(1):1740
De Ramón A, Larraín J (1979) Una metrología colonial para Santiago de Chile: de la medida castellana al sistema métrico decimal. Historia (Santiago: Instituto de Historia, Pontificia Universidad Católica de Chile) 14: 5–71
Rodríguez C, Pérez Y, Moreno H, Clayton J, Antinao J, Duhart P, Martin M (1999) Area de Panguipulli-Riñihue, Región de Los Lagos. Serv Nac Geol Min Mapas Geol, 10(1)
Ruiz S, Madariaga R (2018) Historical and recent large megathrust earthquakes in Chile. Tectonophysics 733:37–56
Sepúlveda SA, Serey A, Lara M, Pavez A, Rebolledo S (2010) Landslides induced by the April 2007 Aysén Fjord earthquake. Chil Patagon Landslides 7(4):483–492. https://doi.org/10.1007/s10346-010-0203-2

Serey A, Piñero-Feliciangeli L, Sepúlveda SA, Poblete F, Petley DN, Murphy W (2019) Landslides induced by the 2010 Chile megathrust earthquake: a comprehensive inventory and correlations with geological and seismic factors. Landslides 16(6):1153–1165. https://doi.org/10.1007/s10346-019-01150-6

Silgado E (1985) Terremotos destructivos en America del Sur: 1530–1894. Centro Regional de Sismología para America del Sur (CERESIS), 10: 328

Solari ME, Cueto C, Hernández F, Rojas JF, Camus P (2011) Procesos territoriales y bosques en la cuenca del río Valdivia (siglos XVI-XIX). Revista Geogr Norte Grande 49:45–62

USGS (2016) M 7.6 - 41km SW of Puerto Quellon, Chile, https://earthquake.usgs.gov/earthquakes/feed/v1.0/detail/us10007mn3.kml

Vanneste K, Wils K, Van Daele M (2018) Probabilistic evaluation of fault sources based on paleoseismic evidence from mass-transport deposits: the example of Aysén Fjord, Chile. J Geophys Res Solid Earth 123:9842–9865. https://doi.org/10.1029/2018JB016289

Watkinson IM, Hall R (2019) Impact of communal irrigation on the 2018 Palu earthquake-triggered landslides. Nat Geosci 12:940–945

Weischet W (1963) Further observations of geologic and geomorphic changes resulting from the catastrophic earthquake of May 1960, in Chile. Bull Seismol Soc Am 53(6):1237–1257

Wils K, Van Daele M, Kissel C, Moernaut J, Schmidt S, Siani G, Lastras G (2020) Seismo-turbidites in Aysén Fjord (southern Chile) reveal a complex pattern of rupture modes along the 1960 megathrust earthquake segment. J Geophys Res Solid Earth 125(9):e2020JB019405

Wright C, Mella A (1963) Modifications to the soil pattern of South-Central Chile resulting from seismic and associated phenomenona during the period May to August 1960. Bull Seismol Soc Am 53(6):1367–1402

Wu W, Sidle RC (1995) A distributed slope stability model for steep forested basins. Water Resour Res 31(8):2097–2110. https://doi.org/10.1029/95wr01136

Zúñiga Álvarez A (2019) Análisis geológico-geotécnico de sedimentos glaciolacustres asociados a los graduales del río San Pedro, Región de Los Lagos. Undergraduate Thesis of University of Chile. Unpublished. Available in https://repositorio.uchile.cl/handle/2250/173836